Ku-Band Low-Noise Amplifier Configuration and Optimization Through BiLSTM-Based Deep Neural Networks

IEEE Access
Multidisciplinary ⋮ Rapid Review ⋮ Open Access Journal

Received 24 February 2026, accepted 14 March 2026, date of publication 17 March 2026, date of current version 20 March 2026.
Digital Object Identifier 10.1109/ACCESS.2026.3674770

RESEARCH ARTICLE

Ku-Band Low-Noise Amplifier Configuration and Optimization Through BiLSTM-Based Deep Neural Networks

LIDA KOUHALVANDI [1], (Senior Member, IEEE), AND LADISLAU MATEKOVITS [2,3,4], (Senior Member, IEEE)
[1]Department of Electrical and Electronics Engineering, Dogus University, 34775 Istanbul, Türkiye
[2]Department of Electronics and Telecommunications, Politecnico di Torino, 10129 Turin, Italy
[3]Department of Measurements and Optical Electronics, Politehnica University Timisoara, 300006 Timişoara, Romania
[4]Istituto di Elettronica e di Ingegneria dell'Informazione e delle Telecomunicazioni, National Research Council, 10129 Turin, Italy
Corresponding author: Ladislau Matekovits (ladislau.matekovits@polito.it)

ABSTRACT This work proposes an automated configuration and sizing framework for a low-noise amplifier (LNA) operating in the Ku-band. The methodology is based on the implementation of deep neural networks (DNNs), specifically a bidirectional long short-term memory (BiLSTM) classifier and a BiLSTM regression model, which are employed sequentially to first generate an appropriate LNA topology and subsequently predict the optimal design parameters of the selected configuration. To further refine the design toward multiple conflicting objectives, a multi-objective multiverse optimization (MOMVO) algorithm is integrated into the workflow to balance key performance metrics such as noise figure, and gain. The overall process is fully automated through the coordinated use of an electronic design automation (EDA) tool and a numerical analysis environment, wherein the circuit topology is synthesized and simulated in the EDA platform, while parameter optimization and decision-making are carried out in the numerical analyzer. This closed-loop framework enables rapid convergence to high-performance solutions with minimal human intervention. The practical effectiveness of the proposed methodology is validated by designing and optimizing an LNA suitable for a Ku-band small satellite receiver, achieving a noise figure below 1.5 dB while satisfying gain and stability constraints, thereby demonstrating the viability of deep learning–assisted automated radio frequency circuit design.

INDEX TERMS Automated, bidirectional long short-term memory (BiLSTM), deep neural network (DNN), low noise amplifier (LNA), Ku-band, multi-objective multi-verse optimization (MOMVO).

I. INTRODUCTION

In the communication systems, low noise amplifiers (LNAs) are the initial devices in satellite transponders that influence on the overall performances of subsequent circuits [1]. The main responsibility of the LNAs is to enhance the received signal effectively to be able to be employed in diverse processes [2]. The noise specification of any LNA can be decreased by appropriately designing circuit topologies along with considering biasing operations. Recently, behavioral modeling with the help of artificial neural networks (ANNs) are developing results in determining relationships between inputs and outputs of any device [3], [4], [5], [6], [7], [8].

In [9] a keyword spotting system is designed which includes an LNA, and the skip-recurrent neural network algorithm that is employed for minimizing the power consumption. The time-domain convolutional neural network (CNN) is presented in [3] which is sampling from the used LNA and the trained ANN leads to adapt features for various applications. For the human movement detection includes the LNA design, in [10] two CNNs are employed for learning features. With the help of these networks, motion classifications are performed for the acceptable accuracy. The deep neural network (DNN) structure is used

The associate editor coordinating the review of this manuscript and approving it for publication was Pedro Miguel Cabral.

in [11] for correcting the high signal distortions, and for inherently robust to noise. In [12], a long-short term memory (LSTM)-based DNN is employed for providing a relationship between the envelope voltage and real angle-of-arrival. This methodology leads to reduce the noise effects. In another study, [13], the DNN is used for LNA circuits and for estimating the proper orthogonal decomposition coefficients. A Siamese-LSTM based network is presented in [14] for modeling the LNA in which transient response is modeled. The CNN model is executed in [15] for reducing noise in the phase-sensitive optical time-domain reflectometry systems results in enhanced signal-to-noise ratio specification. In [16], an automated analog radio frequency (RF) circuit sizing methodology based on a cascade of shallow neural networks (SNNs), targeting RF designs operating in the 2–5 GHz range is presented. Unlike conventional end-to-end deep learning (DL) approaches, the method decomposes the sizing task into a sequence of dedicated SNNs, where each network predicts a single component value and constrains the input space of the subsequent networks. This cascading strategy effectively reduces the dimensionality of the solution space at each step, enabling accurate learning from relatively small training datasets and mitigating the issue of multiple, often impractical, sizing solutions. In another study, [17], an ultra-low-power voice activity detector that integrates analog signal processing with a digital DNN for efficient speech/non-speech classification is presented. The system performs acoustic feature extraction directly in the analog domain at the microphone output using newly designed circuits, including the LNA, bandpass filter, and full-wave rectifier, followed by approximate event-driven analog-to-digital conversion. A three-hidden-layer binarized multilayer perceptron is employed for classification, significantly reducing digital power consumption. In [18], an end-to-end DL framework for multi-pair two-way massive multiple-input multiple-output systems in the presence of nonlinear power amplifier (PA) impairments is investigated. An analytical study of symbol error rate performance over block-fading Rayleigh channels, deriving closed-form expressions that quantify the impact of PA nonlinearity on system reliability is presented. To mitigate PA distortion and multiuser interference, a two-stage precoding strategy is adopted at the relay: a neural network–based transmitter compensates for the PA nonlinearity, followed by a linear zero-forcing precoder to suppress inter-user interference.

This paper presents a two-stage automated methodology for the LNA design, in which the constituent steps are executed sequentially. In the first stage, the optimal LNA configuration is predicted using a classification bidirectional long short-term memory (BiLSTM)–based DNN, which determines the most suitable circuit topology based on the targeted performance specifications. In the second stage, a regression BiLSTM-based DNN is employed to predict the optimal geometric parameters associated with the selected configuration. For the adopted active device, namely a heterojunction field-effect transistor (FET), the complete LNA topology, including the sizing of the input and output matching networks (MNs), is synthesized automatically, culminating in the generation of a ready-to-fabricate layout at the final stage of the design flow.

The employed optimization algorithm is the multi-objective multiverse optimization (MOMVO) technique, which is selected due to its strong capability to converge toward globally optimal solutions in a multi-objective search space [19]. The MOMVO algorithm enables the simultaneous optimization of multiple conflicting performance metrics, such as noise figure (NF), gain, and stability, thereby ensuring a balanced trade-off among key design objectives. The entire optimization process is executed in a fully automated manner through the tight integration of an electronic design automation (EDA) tool and a numerical analysis environment, wherein circuit generation, simulation, and iterative optimization are performed in a closed-loop framework. The effectiveness of the proposed method is validated by designing and optimizing an LNA operating in the Ku-band, with simulation results demonstrating that the achieved performance satisfies stringent noise and gain requirements, thereby confirming the robustness and practicality of the proposed DL–assisted RF design methodology.

This paper is organized as follows: Section II presents the overall methodology used for designing and optimizing an LNA with the help of BiLSTM-based DNNs. Section III explains the simulations results of optimized LNA operating from 12.58 GHz to 13.4 GHz. Finally, Section IV concludes this work.

II. PROPOSED OPTIMIZATION METHOD BASED ON DNNs

A BiLSTM is an advanced recurrent neural network that processes a sequence in both forward and backward directions [20], [21], [22]. The BiLSTM-based layers are used for learning from the complete time series. Here, this type of layers is employed since the outcomes of LNA are in sequence of frequency. With this type of layer, the current output can depend on the past outcome along with capturing long-term dependencies. Hence, each time step can consider the past and future contexts all together. This type of layer will find great solutions for nonlinearity and memory effects concepts which are existing in the amplifier design. With respect to these novelties, the BiLSTM-based layers are used in this work.

The proposed methodology incorporates two BiLSTM–based DNNs that operate sequentially to automate the LNA design process. In the first stage, a BiLSTM-based classification network is utilized to identify the most suitable LNA configuration from a predefined set of candidate topologies, taking into account the targeted performance specifications and design constraints. In the second stage, a BiLSTM-based regression network is employed to predict the optimal geometric values of the circuit components used in both the front-end and back-end MNs, thereby enabling precise control over impedance matching and overall RF performance. The first phase relies on classification-based predictive modeling, whereas the second phase adopts regression-based predictive modeling to map high-level specifications. For accurately modeling the LNA, a suitable amount of data set involves training, validation and test data sets are needed. For this case, the geometric values of employed elements are altered randomly within the various ranges of $\mp 5\%$, $\mp 10\%$, $\mp 15\%$, $\mp 20\%$, and $\mp 25\%$. The generated data set is split into three groups of training, validation, and testing data with the rates of 70%, 15%, 15%, respectively.

This section is devoted to presenting the methodologies employed for constructing and training these networks, including the formulation of the input feature space, the definition of output labels and regression targets, and the selection of appropriate network architectures and hyperparameters. Furthermore, the proposed framework integrates electromagnetic (EM)–verified design variables into the learning process to ensure that the predicted component geometries are physically realizable and consistent with post-layout parasitic effects. By coupling data-driven modeling with EM-aware parameterization, the methodology enables simultaneous optimization of the LNA structure and its associated design variables, thereby improving design accuracy, reducing iteration time, and enhancing the robustness of the synthesized solutions against fabrication and layout-induced variations.

A. CLASSIFICATION PREDICTIVE MODELING WITH BiLSTM-BASED DNN

One of the most significant challenges in the design and optimization of RF amplifiers is the generation of an appropriate initial configuration for the MNs, as this choice has a decisive impact on achievable NF, gain, and stability. Consequently, the first problem of interest in the proposed framework is the accurate prediction of the optimal MN structure. To address this issue, the simplified real frequency technique (SRFT) [23] is first employed to systematically generate a diverse set of candidate MN topologies. In this method, the numerator polynomial defined as $h(\lambda) = h_1\lambda^m + h_2\lambda^{(m-1)} + \ldots + h_m + 1$ plays a central role in producing multiple MN realizations, such as $1\times\ m$ networks for all $m \geq 3$. The initial coefficient matrix is given by $h_0 = [\mp 1 \quad 0]$, which serves as the starting point for the recursive generation of admissible network structures. By applying the SRFT method to the provided S-parameter data of the employed transistor, namely S_{11}, S_{22}, and S_{21} a family of MN configurations corresponding to different values of 'm' is obtained. These configurations represent alternative realizations of input and output MNs. To this end, a classification BiLSTM-based DNN is constructed, comprising an input layer, multiple hidden layers, and a fully connected output layer, as illustrated in Figure 1. The output layer produces categorical labels '1','2',...,'m', corresponding to the respective MN models, thereby enabling data-driven selection of the optimal network structure based on the targeted performance specifications. This classification-driven structural prediction stage effectively reduces the combinatorial search space of feasible MN configurations and provides a robust initialization for the subsequent regression-based parameter optimization stage. By coupling SRFT-based topology synthesis with BiLSTM-based classification DNN, the proposed framework leverages both classical network theory and modern DL to automate the early design phase, improve convergence speed, and enhance the overall reliability of the LNA synthesis process.

In order to effectively train the proposed classification DNN, a sufficiently large and representative dataset must be prepared. For this purpose, the nominal design values corresponding to the various MN models generated through the SRFT method are systematically tuned via random iterative sampling to collect diverse training instances. This randomized exploration of the design space enables the generation of input–output pairs that capture variations in circuit behavior across different configurations, thereby improving the generalization capability of the learning model. Each training sample is labeled according to the associated MN topology index 'm', which serves as the categorical target for the classification task.

For this DNN configuration, a softmax layer is employed as the activation function in the output layer to produce normalized class probabilities over the candidate configurations, while the cross-entropy loss function is used to quantify the discrepancy between the predicted and true class labels during training. After generating a suitable amount of labeled data and defining the activation with loss functions, the hidden-layer architecture is determined through a progressive model-complexity search. Specifically, the number of neurons in each layer and the number of stacked BiLSTM layers are gradually increased to enhance the representational capacity of the network. This architecture exploration is implemented using a MATLAB "for-loop" routine that iteratively trains multiple candidate models and evaluates their classification accuracy on a validation dataset. The process is terminated once a sufficiently high and stable accuracy is achieved, thereby yielding an optimized network architecture that balances prediction performance and computational complexity.

This systematic data-generation and architecture-tuning strategy ensures that the trained BiLSTM classifier can reliably discriminate among alternative MN topologies, providing a robust foundation for the subsequent regression-based stage of the automated LNA design framework.

After completing the training phase of the classification DNN, the recommended data corresponding to the employed transistor are fed into the constructed network as input features. The trained DNN then produces a probability distribution over the possible class labels at the output layer, with each probability reflecting the network's confidence in a particular MN configuration. Among the set of candidate models, the label associated with the highest predicted probability is selected as the optimal configuration and is designated as the winner structure for subsequent stages of the design flow. Moreover, by leveraging the learned nonlinear mapping between transistor characteristics, frequency specifications, and MN structures, the proposed classifier effectively reduces the dependence on exhaustive simulation-based topology searches. The selected winner structure is subsequently passed to the regression BiLSTM-based DNN and the multi-objective optimization module, where fine-grained geometric parameter tuning and performance trade-off optimization are carried out. This hierarchical selection-and-refinement strategy ensures a coherent transition from data-driven structural prediction to physics-aware parameter optimization, thereby enhancing both the efficiency and reliability of the overall automated LNA synthesis framework.

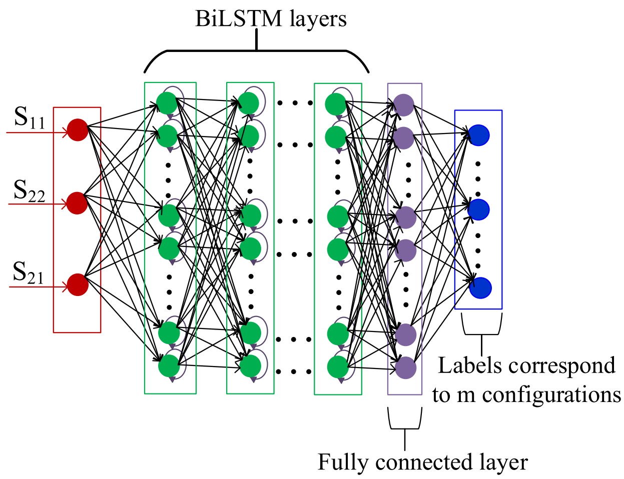

FIGURE 1. Classification BiLSTM-based DNN for predicting the optimal configuration for the LNA design.

B. REGRESSION PREDICTIVE MODELING WITH BiLSTM-BASED DNN

After predicting the optimal configuration, the next stage focuses on obtaining the optimal geometric values through the combined use of a regression-based DNN and the MOMVO algorithm, as illustrated in Figure 2. In this stage, the regression BiLSTM-based DNN serves as a fast surrogate model that captures the nonlinear mapping between the physical design parameters and the corresponding RF performance metrics. The input layer of the network represents the width ('W') and length ('L') of the transmission lines (TLs) employed in the selected MN topology, while the output layer is dedicated to predicting the key circuit responses, namely the S-parameters (S_{11}, S_{12}, S_{21}) along with the NF. This formulation enables the network to directly link geometric design variables to critical performance indicators that govern LNA behavior. The nominated specifications are subsequently optimized through the MOMVO algorithm, which is well suited for multi-objective optimization problems due to its strong global search capability and its effectiveness in improving the coverage and diversity of Pareto-optimal solutions. By simultaneously considering multiple conflicting objectives—such as minimizing NF and input reflection while maximizing gain—the MOMVO-driven search process refines the DNN-predicted design parameters toward balanced, high-performance solutions. In this hybrid framework, the regression DNN accelerates performance evaluation, while MOMVO guides the exploration of the design space,

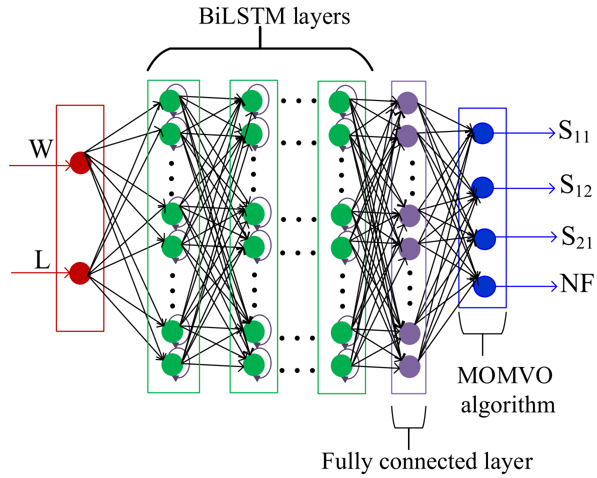

FIGURE 2. Regression BiLSTM-based DNN for estimating the optimal geometric values of selected topology predicted by classification DNN.

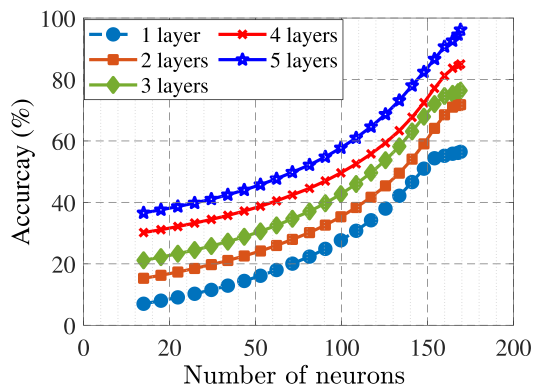

FIGURE 3. Accuracy of the trained classification BiLSTM-based DNN.

M.1 73%	M.2 78%	M.3 81%	M.4 80%
M.5 70%	M.6 85%	M.7 77%	M.8 79%
M.9 89%	M.10 83%	M.11 74%	M.12 81%
M.13 80%	M.14 85%	M.15 92%	M.16 96%

FIGURE 4. Various models (donated as 'M') generated by the SRFT model and the probability estimated by the classification DNN as the confusion matrix for each model.

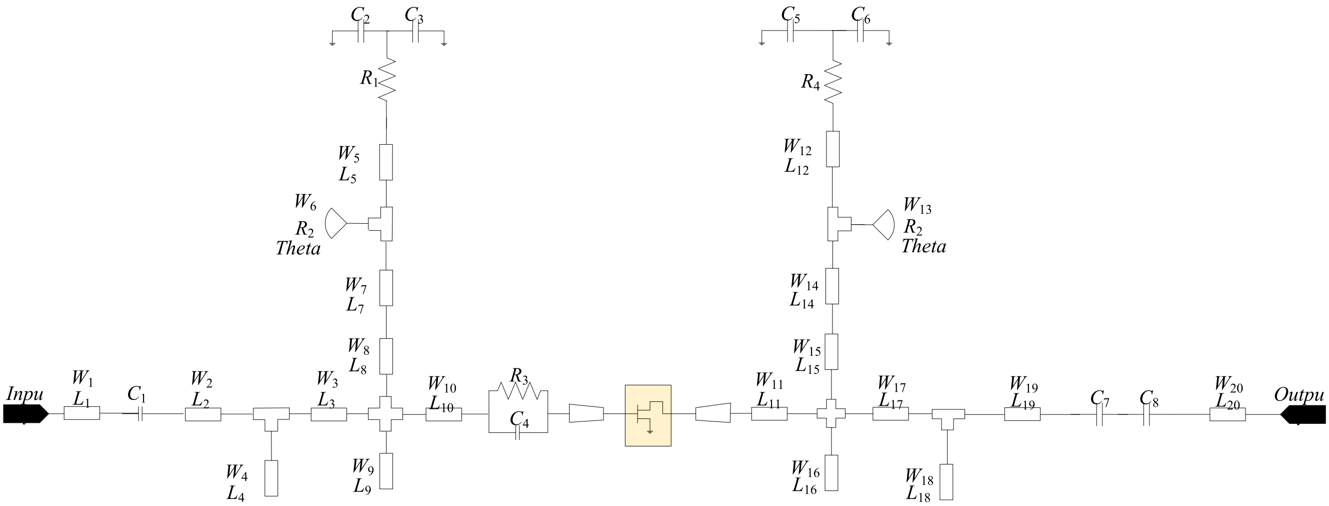

FIGURE 5. Optimized LNA through the proposed methodologies.

thereby significantly reducing the computational burden associated with circuit-level simulations.

For this regression network, the rectified linear unit (ReLU) function is employed as the activation function in the hidden layers to enhance nonlinear modeling capability and mitigate vanishing-gradient issues, while the mean squared error (MSE) is adopted as the loss function to quantify the discrepancy between predicted and target performance metrics during training. A sufficiently large and diverse training dataset is generated by randomly iterating the TL component values within variation ranges of 5%, 10%, and 15% around their nominal values. This controlled strategy ensures that the training samples adequately span the local design space, improves the robustness of the learned regression model against fabrication tolerances, and enhances its generalization capability for unseen design instances. By integrating regression-based DL with MOMVO-driven multi-objective optimization, the proposed framework enables efficient and accurate prediction of optimal geometric parameters, providing a seamless transition from topology selection to fine-grained circuit sizing in the automated LNA design flow.

III. PRACTICAL EXECUTION OF VARIOUS DNNs WITH THE SIMULATION RESULTS

As discussed in the preceding sections, the proposed methodology is fully automated through the tight integration of NI AWR Design Environment with MATLAB, wherein the LNA circuit is synthesized and simulated in the AWR tool, and the corresponding performance data are programmatically extracted and processed in MATLAB to enable the deployment of the proposed DL and optimization algorithms. In this co-simulation framework, MATLAB serves as the numerical analyzer that manages data generation, DNN training, topology prediction, and multi-objective optimization implementation, while NI AWR provides accurate circuit-level and EM simulation capabilities for performance verification. This bidirectional communication between the two platforms establishes a closed-loop design flow that minimizes manual intervention and significantly accelerates the overall synthesis process.

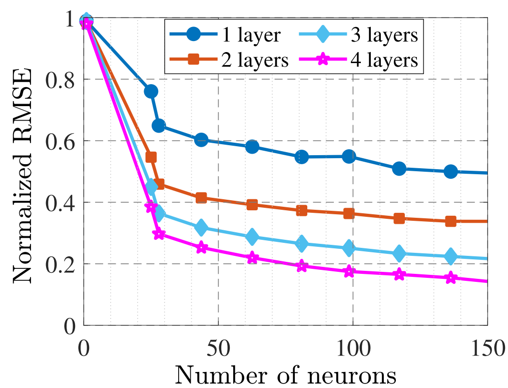

FIGURE 6. Accuracy of trained regression BiLSTM-based DNN.

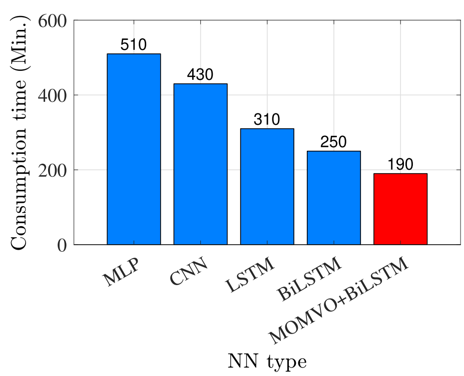

FIGURE 7. Consumption time of LNA design with various types of NN.

All computational tasks are executed on a workstation equipped with an Intel Core i7-4790 CPU operating at

TABLE 1. Values of LNA structure presented in Figure 5 for before and after optimization; W/L is in mm, capacitors (c) are in PF and resistors (R) are in Ω units.

Design parameters	Before optimization	After optimization	Design parameters	Before optimization	After optimization
W_1/L_1	1.2/2.3	1.93/2.0	W_{17}/L_{17}	1.0/2.3	1.93/2.0
W_2/L_2	1.13/2.3	1.93/2.0	W_{18}/L_{18}	1.4/2.3	0.72/2.5
W_3/L_3	2.0/1.3	1.93/3.1	W_{19}/L_{19}	1.6/2.0	1.93/4.3
W_4/L_4	0.6/2.8	0.65/1.5	W_{20}/L_{20}	0.8/2.3	1.93/2.0
W_5/L_5	0.40/2.66	0.80/2.0	R_1	0.6	10
W_6	0.44	0.55	R_2	0.6	5
W_7/L_7	1.43/1.2	0.80/1.2	R_3	1.5	10
W_8/L_8	0.80/2.3	0.30/2.0	R_4	210	300
W_9/L_9	0.36/0.80	0.8/0.65	C_1	3.3	1
W_{10}/L_{10}	0.80/2.4	1.93/2.5	C_2	50	220
W_{11}/L_{11}	1.20/2.3	1.93/3.4	C_3	150	220
W_{12}/L_{12}	0.46/2.3	0.80/2.0	C_4	0.8	0.1
W_{13}	0.36	0.55	C_5	100	4700
W_{14}/L_{14}	0.58/2.3	0.80/2.0	C_6	160	220
W_{15}/L_{15}	0.78/2.3	0.30/3.5	C_7	2.2	1
W_{16}/L_{16}	0.80/2.3	0.80/0.80	C_8	1.1	1.5
$Theta$	45	45	-	-	-

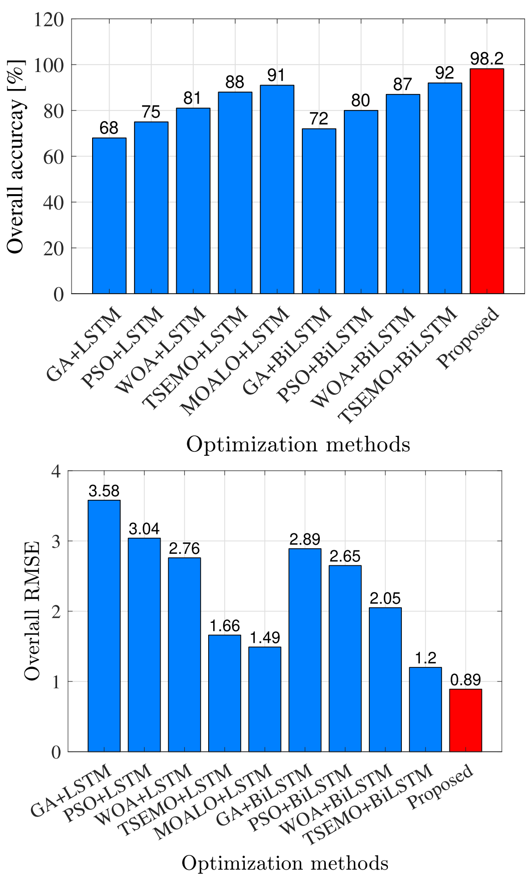

FIGURE 8. Performance comparison by the utilization of LSTM hidden layers versus BiLSTM hidden layers with various optimization methods; classification DNN (top), and regression DNN (bottom).

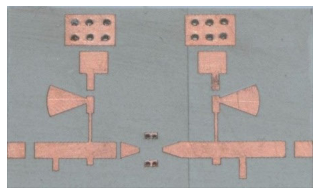

FIGURE 9. Layout of fabricated LNA.

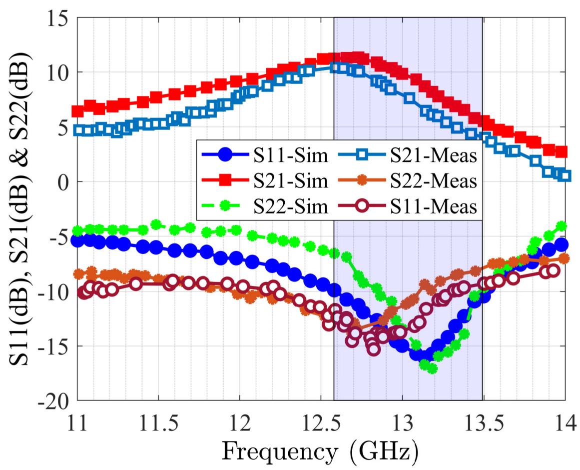

FIGURE 10. Simulated (Sim) and measurement (Meas) S-parameter performances of optimized LNA.

3.60 GHz and 32.0 GB of RAM, which ensures sufficient processing power for iterative DNN training, large-scale data handling, and repeated optimization cycles. Using the proposed automated framework, the LNA operating in the Ku-band is successfully designed and optimized, ultimately resulting in a ready-to-fabricate layout. These results demonstrate the practical feasibility and robustness of the proposed DL–assisted LNA design methodology, as well as its potential to streamline RF front-end development for high-frequency satellite communication applications.

As the first step of the proposed design flow, the NEC NE3511S02 heterojunction field-effect transistor (HJ-FET) is selected as the active device for designing the LNA circuit operating in the Ku-band [24]. This transistor is chosen due to its favorable high-frequency characteristics and low-noise

TABLE 2. Summary of various reported ML techniques in the literature.

Ref.	Method	Goal(s)	Summary of work
[26]	Behavior modeling of PA	Presenting an optimal DNN model for PA	DNN construction for the PA in which the input specifications are in-phase and quadrature-phase (I/Q) components
[27]	Presenting a residual selectable modeling method to achieve the residual DNN	Constructing the multistate PA behavioral model	DNN construction for the PA with I/Q components and improving the modeling accuracy
[28]	Implementation of CNN-based surrogate model	Designing a Class F PA through pixelated layout configuration	Obtaining output power of 41.6 dBm and a drain efficiency of 74% at 2.9 GHz
[16]	Utilization of shallow neural network in cascade form	Sizing CMOS-based analog-radio frequency designs	Accelerating circuit sizing
[29]	Utilization of recurrent neural network (RNN)	Behavioral modeling along with digital predistortion of PA	Results in acceptable linearization
[30]	Implementation of BiLSTM-based networks	Characterization and linearization of PA with DPD method	Presenting a promising linearization performance
[31]	Utilization of multi-channel convolutional long short-term deep neural network	Constructing the behavioral modeling of PA	Presenting acceptable adjacent channel error power ratio
This work	**Utilization of two BiLSTM-based DNNs along with the MOMVO algorithm**	**- Predicting the optimal PA topology with classification; - PA sizing through regression BiLSTM-based DNN - Utilization of multi-objective optimization for improving the overall performance**	**Accelerating the PA design more effectively and fully automatically**

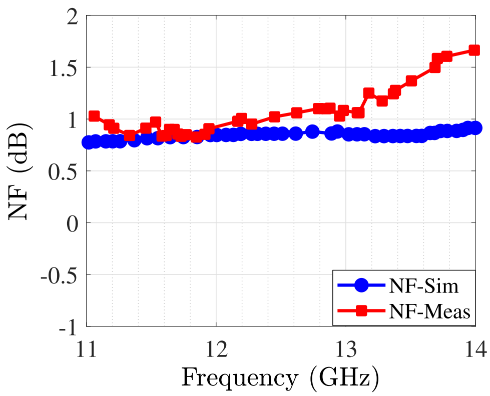

FIGURE 11. NF specification of optimized LNA.

performance, which make it suitable for satellite receiver front-end applications. The S-parameter specifications of the device are provided as inputs to the simplified real frequency technique (SRFT), resulting in the systematic generation of 16 different MN configurations. Each of these configurations represents a different candidate topology for the input and output MNs of the LNA.

For each of the 16 generated structures, random iterative tuning is performed and corresponding S-parameter responses are arranged, thereby creating a diverse dataset for training the classification network. Through this process, a total of $16 \times 100 = 1600$ sequential data samples as multi-segment data are generated, where each sample comprises a set of input features derived from the circuit parameters and the associated performance metrics. The output response of each data sample is categorized into one of m=16 class labels, corresponding to the respective SRFT-generated MN configurations. Figure 3 illustrates the classification accuracy of the trained BiLSTM-based DNN as a function of network complexity. It is observed that the optimal performance is achieved with a hidden-layer configuration consisting of five BiLSTM layers and 170 neurons per layer, at which point the classification accuracy reaches 98.2%. This result indicates that the proposed network architecture is capable of reliably discriminating among alternative MN topologies based on the transistor characteristics and circuit response data.

As shown in Figure 4, the SRFT method generates 16 different candidate models for the selected transistor, and the trained classification DNN predicts that the 16th model, depicted in Figure 5, has the highest posterior probability of fitting the characteristics of the employed HJ-FET. Consequently, this model is selected as the optimal LNA configuration and is forwarded to the subsequent regression and multi-objective optimization stages. This data-driven selection of the winner structure effectively eliminates the need for exhaustive topology-level simulations and provides a robust initialization point for fine-grained geometric optimization in the later phases of the proposed automated LNA design framework.

After predicting the optimal structure, a regression BiLSTM-based DNN is constructed to optimize the component values associated with the selected LNA topology shown in Figure 5. For this chosen configuration, the 'W' and 'L' of the TLs are systematically varied to generate a comprehensive training dataset. In total, 2500 data samples are prepared by randomly iterating the TL geometrical parameters within predefined bounds, and the corresponding circuit responses are obtained through simulations. This dataset is subsequently used to train the regression DNN to learn the nonlinear mapping between the physical design variables and the resulting RF performance metrics.

During the training and optimization process, the MOMVO algorithm is integrated at the output stage to guide the search toward globally optimal solutions that simultaneously satisfy multiple performance objectives. In particular, the MOMVO is employed to refine the DNN-predicted parameters so as to optimize the overall LNA performance in terms of key figures of merit, including the S-parameters and the NF specification. This hybrid DNN–MOMVO framework enables efficient exploration of the continuous design space while avoiding the computational overhead associated with exhaustive simulations. Figure 6 illustrates the prediction accuracy of the constructed regression DNN for different network configurations. It is observed that when the number of hidden layers is set to four and each layer consists of 150 neurons, the network achieves its best performance, yielding a root mean square error (RMSE) of 0.89. This result indicates that the selected network architecture provides an effective trade-off between modeling accuracy and computational complexity. With the aid of this trained regression model, the optimal design parameters of the LNA are obtained and are summarized in Tab. 1. Figure 7 describes the effectiveness of the BiLSTM-based DNN with the multi-objective method in minimizing the design consumption time. This figure presents the comparison with various neural networks (NNs) such as multilayer perceptron (MLP), CNN, and LSTM-based NNs. From another point of view for proving the effectiveness of the BiLSTM structure, a comparison between the utilization of LSTM versus BiLSTM-based hidden layers are executed in Fig. 8 with various optimization methods such as genetic algorithm (GA), particle swarm optimization (PSO), whale optimization algorithm (WOA), and thompson sampling efficient multiobjective optimization (TSEMO) [25]. As it is obvious for the two different models of classification and regression networks, the BiLSTM-based configurations result in more improved performances.

For the physical realization of the optimized LNA, a Rogers RO3003 substrate with a thickness of 0.76 mm is employed due to its low dielectric loss and suitability for high-frequency Ku-band applications. The amplifier is biased at 2 V and 10 mA, ensuring stable operation within the desired region of the selected HJ-FET device. These implementation details, together with the DNN–MOMVO-optimized component values, demonstrate the practical feasibility of the proposed automated sizing methodology and its effectiveness in delivering a ready-to-fabricate Ku-band LNA design.

The fabricated layout of optimized LNA is presented in Figu. 9. Figures 10 and 11 present the simulated along with the measurement performance outcomes of the optimized LNA obtained through the proposed DL–assisted design framework. As shown in Figure 10, the optimized LNA exhibits satisfactory impedance matching and gain characteristics over the frequency range from 12.58 GHz to 13.49 GHz, which effectively covers the targeted Ku-band operating region. Within this band, the input reflection coefficient (S_{11}) remains below the commonly accepted −10 dB threshold, indicating good input matching, while the forward transmission coefficient (S_{21}), demonstrates stable and sufficiently high gain across the bandwidth. At the same time, the reverse isolation (S_{12}) is maintained at a low level, confirming the stability and unilateral behavior of the amplifier.

Figure 11 illustrates the corresponding noise performance of the optimized design, where the NF remains below 1 dB throughout the operating band. This ultra-low noise performance highlights the effectiveness of the proposed regression DNN–MOMVO optimization strategy in accurately tuning the MNs to achieve near-optimal noise matching conditions. The simultaneous satisfaction of stringent noise and gain specifications demonstrates that the proposed methodology is capable of balancing multiple conflicting objectives. These results collectively confirm that the optimized LNA meets the key performance requirements for Ku-band small-satellite receiver front-end applications. Additionally to underline the novelty of the proposed method, Tab. 2 is presented.

IV. CONCLUSION

In this work, a DNN–based framework employing BiLSTM hidden layers for the automated design and optimization of the LNA is presented. The entire methodology is executed in a fully automated manner, minimizing manual intervention and significantly reducing design iteration time. The proposed approach is structured into two main phases: (i) the prediction of the optimal MN configuration and (ii) the estimation and optimization of the corresponding geometric design parameters. In the first phase, a classification DNN is employed to identify the optimum MN topology that best fits the characteristics of the selected transistor, primarily based on its S-parameter behavior. In the second phase, a regression DNN is utilized to optimize the widths and lengths of the TLs, and its predictions are further refined through the MOMVO algorithm. This hybrid regression–optimization strategy enables the simultaneous enhancement of key RF performance metrics, including S-parameters and NF, while maintaining a balanced trade-off among conflicting design objectives. By integrating EM–verified design variables and multi-objective optimization into the learning framework, the proposed method ensures that the synthesized solutions are both physically realizable and performance-optimal. The presented framework is flexible and scalable, allowing it to be adapted to different transistor technologies, frequency bands, and performance specifications. It substantially reduces the dependency on designers' empirical experience and domain-specific heuristics through a closed-loop interaction between the EDA environment and the numerical analyzer. The effectiveness and practical feasibility of the proposed methodology are verified by designing and optimizing an LNA operating in the Ku-band frequency range, with simulation results demonstrating compliance with stringent noise and gain requirements. These outcomes confirm that DL–assisted automation represents a promising paradigm for next-generation RF front-end design, particularly for high-frequency and multi-objective optimization scenarios.

REFERENCES

[1] C. Wang, J. Yang, Y. Li, Z. Wang, H. Jie, Z. Zheng, Z. Zhao, Z. Shu, and Y. Guo, "A spike-driven transformer network for edge computing-based partial discharge monitoring using ultrahigh frequency pulse signals," *IEEE Trans. Microw. Theory Techn.*, vol. 73, no. 10, pp. 8071–8082, Oct. 2025.

[2] J. Xu, Y. Shen, J. Deng, E. Chen, and V. Chen, "A reinforcement-learning-assisted power amplifier for RF fingerprint generation in 65 nm CMOS," *IEEE Trans. Circuits Syst. I, Reg. Papers*, vol. 71, no. 7, pp. 3050–3063, Jul. 2024.

[3] F. Chen, K.-F. Un, W.-H. Yu, P.-I. Mak, and R. P. Martins, "A 108-nW 0.8-mm2 analog voice activity detector featuring a time-domain CNN with sparsity-aware computation and sparsified quantization in 28-nm CMOS," *IEEE J. Solid-State Circuits*, vol. 57, no. 11, pp. 3288–3297, Nov. 2022.

[4] R. Zhang, X. Cen, K.-F. Un, M. Guo, L. Qi, R. P. Martins, and S.-W. Sin, "A 362-TOPS/W mixed-signal MAC macro with sampling-weight-nonlinearity cancellation and dynamic-amplified accumulation," *IEEE Trans. Circuits Syst. I, Reg. Papers*, vol. 72, no. 7, pp. 3059–3071, Jul. 2025.

[5] D.-H. Han, X.-C. Wei, and R. X.-K. Gao, "A field reconstruction method for EMI near-field scanning based on wave equation-informed neural network," *IEEE Trans. Instrum. Meas.*, vol. 74, pp. 1–8, 2025.

[6] J. He and J. He, "A grouped-ANN equalizer for the rotated PS 64QAM OFDM in W-band ROF system," *IEEE Photon. Technol. Lett.*, vol. 36, no. 19, pp. 1165–1168, Aug. 30, 2024.

[7] S. Zhou, Z. Li, L. Cheng, J. Hadorn, C. Gao, Q. Chen, T. Delbruck, K. Kim, and S.-C. Liu, "An 8.62-μW 75-dB DR SoC fully integrated SoC for spoken language understanding," *IEEE J. Solid-State Circuits*, vol. 60, no. 11, pp. 4002–4017, Nov. 2025.

[8] J. Kim, B. Seo, Y. H. Oh, J.-H. Chun, J. W. Lee, and J. Kim, "An 8-bit ring-amplifier based mixed-signal MAC circuit with full digital interface and variable accumulation length," *IEEE Access*, vol. 9, pp. 5887–5894, 2021.

[9] H. Yang, J.-H. Seol, R. Rothe, Z. Fan, Q. Zhang, H.-S. Kim, D. Blaauw, and D. Sylvester, "A 1.5-μW fully-integrated keyword spotting SoC in 28-nm CMOS with skip-RNN and fast-settling analog frontend for adaptive frame skipping," *IEEE J. Solid-State Circuits*, vol. 59, no. 1, pp. 29–39, Jan. 2024.

[10] H. Arab, I. Ghaffari, L. Chioukh, S. O. Tatu, and S. Dufour, "A convolutional neural network for human motion recognition and classification using a millimeter-wave Doppler radar," *IEEE Sensors J.*, vol. 22, no. 5, pp. 4494–4502, Mar. 2022.

[11] Y. Zhang, Z. Wang, Y. Huang, W. Wei, G. F. Pedersen, and M. Shen, "A digital signal recovery technique using DNNs for LEO satellite communication systems," *IEEE Trans. Ind. Electron.*, vol. 68, no. 7, pp. 6141–6151, Jul. 2021.

[12] Y. Li, Q. Cai, J. Yang, T. Zhou, Y. Peng, and T. Jiang, "A novel deep learning-assisted microwave photonic direction finding system based on long-baseline array," *J. Lightw. Technol.*, vol. 41, no. 15, pp. 4971–4978, Mar. 6, 2023.

[13] Z. Li, Z.-M. Wu, X.-C. Li, S.-P. Gao, Y.-X. Guo, and J.-F. Mao, "A POD-enhanced multi-PCE DNN for high-dimensional uncertainty quantification of high-speed circuits," *IEEE Trans. Microw. Theory Techn.*, vol. 73, no. 8, pp. 4468–4479, Aug. 2025.

[14] G. Zhang and W. Huang, "Advancing circuit transient response macromodeling: From conventional neural networks to siamese-LSTM," *IEEE Trans. Circuits Syst. I, Reg. Papers*, vol. 71, no. 12, pp. 6166–6176, Dec. 2024.

[15] S. Li, K. Liu, J. Jiang, T. Xu, Z. Ding, Z. Sun, Y. Huang, K. Xue, X. Jin, and T. Liu, "An ameliorated denoising scheme based on deep learning for Φ-OTDR system with 41-km detection range," *IEEE Sensors J.*, vol. 22, no. 20, pp. 19666–19674, Oct. 2022.

[16] P.-O. Beaulieu, É. Dumesnil, F. Nabki, and M. Boukadoum, "Analog RF circuit sizing by a cascade of shallow neural networks," *IEEE Trans. Comput.-Aided Design Integr. Circuits Syst.*, vol. 42, no. 12, pp. 4391–4401, Dec. 2023.

[17] M. Yang, C.-H. Yeh, Y. Zhou, J. P. Cerqueira, A. A. Lazar, and M. Seok, "Design of an always-on deep neural network-based 1-μ w voice activity detector aided with a customized software model for analog feature extraction," *IEEE J. Solid-State Circuits*, vol. 54, no. 6, pp. 1764–1777, Jun. 2019.

[18] M. Cherif, A. Arfaoui, R. Zayani, and R. Bouallegue, "End-to-end deep learning for multipair two-way massive MIMO with PA impairments," *IEEE Syst. J.*, vol. 17, no. 2, pp. 3150–3159, Jun. 2023.

[19] S. Mirjalili, P. Jangir, S. Z. Mirjalili, S. Saremi, and I. N. Trivedi, "Optimization of problems with multiple objectives using the multi-verse optimization algorithm," *Knowledge-Based Syst.*, vol. 134, pp. 50–71, Oct. 2017. [Online]. Available: https://www.sciencedirect.com/science/article/pii/S0950705117303404

[20] M. Woźniak, M. Wieczorek, and J. Siłka, "BiLSTM deep neural network model for imbalanced medical data of IoT systems," *Future Gener. Comput. Syst.*, vol. 141, pp. 489–499, Apr. 2023. [Online]. Available: https://www.sciencedirect.com/science/article/pii/S0167739X22004095

[21] L. Chen, X. Lin, L. Ma, and C. Wang, "A BiLSTM model enhanced with multi-objective arithmetic optimization for COVID-19 diagnosis from CT images," *Sci. Rep.*, vol. 15, no. 1, p. 10841, Mar. 2025, doi: 10.1038/s41598-025-94654-2.

[22] M. Kowsher, A. Tahabilder, M. Z. I. Sanjid, N. J. Prottasha, M. S. Uddin, M. A. Hossain, and M. A. K. Jilani, "LSTM-ANN & BiLSTM-ANN: Hybrid deep learning models for enhanced classification accuracy," *Proc. Comput. Sci.*, vol. 193, pp. 131–140, Jul. 2021. [Online]. Available: https://www.sciencedirect.com/science/article/pii/S1877050921020548

[23] S. Yarman, *Design of Ultra Wideband Power Transfer Networks*. New York, NY, USA: Wiley, 2010.

[24] L. Kouhalvand, O. Ceylan, S. Paker, and H. B. Ya, "Design and realization of a novel planar array antenna and low power LNA for Ku-band small satellite communications," *Turkish J. Elect. Eng. Comput. Sci.*, vol. 25, no. 2, pp. 1394–1403, 2017.

[25] S. Li, H. Chen, M. Wang, A. A. Heidari, and S. Mirjalili, "Slime mould algorithm: A new method for stochastic optimization," *Future Gener. Comput. Syst.*, vol. 111, pp. 300–323, Oct. 2020. [Online]. Available: https://www.sciencedirect.com/science/article/pii/S0167739X19320941

[26] X. Yu, X. Hu, Z. Liu, C. Wang, W. Wang, and F. M. Ghannouchi, "A method to select optimal deep neural network model for power amplifiers," *IEEE Microw. Wireless Compon. Lett.*, vol. 31, no. 2, pp. 145–148, Feb. 2021.

[27] Z. Chang, X. Hu, B. Li, Q. Yao, Y. Yao, W. Wang, and F. M. Ghannouchi, "A residual selectable modeling method based on deep neural network for power amplifiers with multiple states," *IEEE Microw. Wireless Technol. Lett.*, vol. 34, no. 8, pp. 1043–1046, Aug. 2024.

[28] H. Zhou, H. Chang, D. Widén, L. Fornstedt, G. Melin, and C. Fager, "AI-assisted deep-learning-based design of high-efficiency class f power amplifiers," *IEEE Microw. Wireless Technol. Lett.*, vol. 35, no. 6, pp. 690–693, Jun. 2025.

[29] A. Fischer-Bühner, L. Anttila, M. Turunen, M. Dev Gomony, and M. Valkama, "Augmented phase-normalized recurrent neural network for RF power amplifier linearization," *IEEE Trans. Microw. Theory Techn.*, vol. 73, no. 1, pp. 412–422, Jan. 2025.

[30] J. Sun, W. Shi, Z. Yang, J. Yang, and G. Gui, "Behavioral modeling and linearization of wideband RF power amplifiers using BiLSTM networks for 5G wireless systems," *IEEE Trans. Veh. Technol.*, vol. 68, no. 11, pp. 10348–10356, Nov. 2019.

[31] R. Li, Z. Yao, Y. Wang, Y. Lin, T. Ohtsuki, G. Gui, and H. Sari, "Behavioral modeling of power amplifiers leveraging multi-channel convolutional long short-term deep neural network," *IEEE Trans. Veh. Technol.*, vol. 74, no. 7, pp. 11456–11460, Jul. 2025.

LIDA KOUHALVANDI (Senior Member, IEEE) received the B.Sc. degree in electronics engineering from the Azad University of Tabriz, Tabriz, Iran, in 2011, the M.Sc. and Ph.D. (Hons.) degrees in electronics engineering from the Istanbul Technical University, Istanbul, Türkiye, in 2015 and 2021, respectively, and the Associate Professor degree, in February 2023. She joined the Department of Electrical and Electronics Engineering, Dogus University, in October 2021, as an Assistant Professor. In recognition of her research, she received the Doctoral Fellowship at the Department of Electronics and Telecommunications, Politecnico di Torino, Turin, Italy, from 2019 to 2020, and also she joined to Politecnico di Torino, as a Research Fellowship, from February 2021 to July 2021 and from May 2022 to May 2023. Her research interests include radio frequency and analog engineer are power amplifier, antenna, analog designs, and implantable medical devices. She also has experience in computer-aided designs and optimization algorithms through machine learning. She received the "Best Presentation Award" from EExPolytech-2021: Electrical Engineering and Photonics Conference in 2021. Additionally, her Ph.D. thesis accepted for the presentation at Ph.D. Forum of the 2021 IEEE/ACM Design Automation Conference (DAC 2021) in San Francisco, USA. From the 30th IEEE Conference on Signal Processing and Communications Applications, she received another "Best Paper Award" in 2022. She received the 2022 Mojgan Daneshmand Grant from the IEEE Antennas and Propagation Society (AP-S), organized by the IEEE AP-S Young Professionals. Additionally, her Ph.D. thesis was awarded by Istanbul Technical University as the "Outstanding Ph.D. Thesis" and also from Turkish Electronics Industrialists Association (TESID) as the "Best Innovation and Creativity Ph.D. Thesis" in 2022.

LADISLAU MATEKOVITS (Senior Member, IEEE) received the degree in electronic engineering from the Institutul Politehnic din Bucureşti, Bucharest, Romania, in 1992, and the Ph.D. degree (Dottorato di Ricerca) in electronic engineering from the Politecnico di Torino, Turin, Italy, in 1995.

Since 1995, he has been with the Department of Electronics and Telecommunications, Politecnico di Torino, first with a post-doctoral fellowship, then as a Research Assistant. He joined the Department of Electronics and Telecommunications as an Assistant Professor, in 2002, and was appointed as a Senior Assistant Professor, in 2005, and as an Associate Professor, in 2014. In February 2017, he obtained a Full Professor qualification in Italy. In late 2005, he was a Visiting Scientist at the Antennas and Scattering Department, FGAN-FHR (now Fraunhofer Institute), Wachtberg, Germany. In July 2009, for two years he has been a Marie Curie Fellow at Macquarie University, Sydney, NSW, Australia, where he also held a visiting academic position, in 2013, and appointed as an Honorary Fellow, in 2014. Since 2020, he has been an Honorary Professor at the Polytechnic University of Timisoara, Romania, and an Associate Researcher with Italian National Research Council. He has been invited to serve as the Research Grant Assessor for government funding calls (Romania, Italy, Croatia, and Kazakhstan) and as the International Expert in Ph.D. thesis evaluation by several Universities from Australia, India, Pakistan, and Spain. In the last years, bio-electromagnetic aspects have also been contemplated, as for example design of implantable antennas or development of nano-antennas for example for drug delivery applications. He has published more than 500 articles, including more than 145 journal contributions, and delivered seminars on these topics all around the world: Europe, USA (AFRL/MIT-Boston), Australia, China, and Russia. His main research activities concern numerical analysis of printed antennas and in particular development of new, numerically efficient full-wave techniques to analyze large arrays, optimization techniques, and active and passive metamaterials for cloaking applications. Material parameter retrieval of these structures by inverse methods and different optimization techniques have also been considered.

Prof. Matekovits has been a member of the Organizing Committee of the International Conference on Electromagnetics in Advanced Applications (ICEAA), since 2010, and he is a member of the technical program committees of several conferences. He was a recipient of various awards in international conferences, including the 1998 URSI Young Scientist Award in Thessaloniki, Greece, the Barzilai Award 1998 (Young Scientist Award, granted every two years by Italian National Electromagnetic Group), and the Best AP2000 Oral Paper on Antennas, ESA-EUREL Millennium Conference on Antennas and Propagation in Davos, Switzerland. He was a recipient of the Motohisa Kanda Award 2018, for the Most Cited Paper of IEEE Transactions on Electromagnetic Compatibility in the past five years, and more recently he has been awarded with the 2019 American Romanian Academy of Arts and Sciences (ARA) Medal of Excellence in Science and by the Ad Astra Award 2020, Senior Researcher, for Excellence in Research. He serves as a reviewer for different journals. He has been the Assistant Chairperson and the Publication Chairperson of European Microwave Week 2002 (Milan, Italy), and the General Chair of the 11th International Conference on Body Area Networks (BodyNets) 2016. He serves as an Associated Editor for IEEE ACCESS, IEEE ANTENNAS AND WIRELESS PROPAGATION LETTERS, and IET MAP.